Journal of Catalysis 298 (2013) 70–76

Contents lists available at SciVerse ScienceDirect

Journal of Catalysis

journal homepage: www.elsevier.com/locate/jcat

Multilple host–guest interactions in heterogeneous vanadium catalysts: Inorganic nanosheets modified alpha-amino acids as ligands

Hui Liu, Liwei Zhao, Jiuzhao Wang, Jing He *

State Key Laboratory of Chemical Resource Engineering, Beijing University of Chemical Technology, Beijing 100029, China

ARTICLE INFO

Article history:
Received 4 September 2012
Revised 16 November 2012
Accepted 17 November 2012

Keywords:
Host–guest interaction
Inorganic nanosheet
α-Amino acid
Supramolecular catalysts

ABSTRACT

The catalysts using layered double hydroxide (LDH) nanosheet-modified α-amino acid anions as ligands has been proved to be easily recycled in vanadium-catalyzed asymmetric epoxidation of cinnamyl alcohol with the enantioselectivity well preserved and the yield only slightly reduced. The α-amino acids employed here include L-glutamate, L-alanine, and L-serine, which are anchored to LDH layers through monodentate electrostatic interactions in the ascending intensity while coordinated with vanadium center in the coordinating intensity of L-glutamate > L-serine > L-alanine. The stronger coordination with α-amino acid anion caused the vanadium center to be leached independently in less percentage, while the leaching of α-amino acid anion depends on the dual host–guest interactions. In nanosheet-modified L-glutamate system, all of the vanadium centers leached together with L-glutamate, but in nanosheet-modified L-alanine system, all of the vanadium centers leached independently. The electrostatic interaction of brucite-like layer with L-serine is stronger than with L-alanine, yet the stronger coordination of L-serine to vanadium caused more L-serine to be leached. The weakest electrostatic interactions between intercalated L-glutamate and LDH layer result in the visible loss of L-glutamate in the vanadium/LDH nanosheet-modified L-glutamate system, but the V-glutamate species leached into the solution was catalytically active in the epoxidation, compensating for the activity loss in the recycling experiments in spite of the higher L-glutamate leaching.

1. Introduction

Elaborate design of efficient and recoverable heterogeneous asymmetric organo-metallic catalyst is of great importance to both fine chemical and pharmaceutical industries with more and more urgent requirement for green chemistry and life safety [1–4]. Typically, two strategies are often considered as effective to immobilize homogeneous metal complexes on a non-soluble support [5,6]. One is "ligand-exchange", in which the chiral ligand is pre-immobilized on the support and then anchored with metal center [7–9]. Another is direct "tethering" of chiral metal complexes to the support [10–13]. In either of the two methods, the host–guest interactions between the ligand and support are very important to catalytic efficiency and catalyst stability. The ligand can be anchored by covalent linkages [14–16] or non-covalent interactions [17–19]. The non-covalent interactions include electrostatic adsorption, encapsulation within the micropores of a zeolite, and entrapment into nanopores of a mesoporous material. Compared with covalent linkages, non-covalent interactions avoid excess modifications of available chiral ligands, which not only preserve the original asymmetric environment but also preclude any inevitable supplementary costs [17]. Unfortunately, non-covalent interactions are not always strong enough to prevent the dissociation of chiral ligands, which gives rise to leaching of metal complexes in the successive catalytic runs. Fraile's group described clay-supported chiral Mn(salen) complexes, which exhibited declined catalytic activity and enantioselectivity after each recovery and mainly in the last recycle as a result of disengagement of the salen ligand from the clay support [20]. Besides, the metal center itself might be leached due to the disassociation of ligand–metal linkage by competitive coordination of by-products, substrate, or solvent molecules. Totviso's group reported the chiral azabis(oxazoline)–cooper complexes immobilized on a silica modified with tungstophosphate $\left(PW_{12}O_{40}^{3-}\right)$ and observed a significant drop in activity and enantioselectivity in continuing catalytic runs because of the deactivation by by-products [13]. Therefore, how to engineer a recoverable asymmetric organo-metallic catalyst by modulating the host–guest interactions is still a great challenge.

In our previous work [21], a simple but vigorous strategy has been proposed to design a valid heterogeneous asymmetric catalyst, in which the pristine α-amino acids were first attached to inorganic nanosheets of layered double hydroxides (LDHs) and then coordinated to vanadium sites. The chiral α-amino acids act

* Corresponding author. Address: Box 98, 15 Beisanhuan Dong Lu, Beijing 100029, China. Fax: +86 10 64425385.
E-mail address: jinghe@263.net.cn (J. He).

0021-9517/$ - see front matter © 2012 Published by Elsevier Inc.
http://dx.doi.org/10.1016/j.jcat.2012.11.022

as the guest of inorganic nanosheets, while vanadium centers are the guest of the chiral α-amino acids attached to nanosheets. The resulting catalysts proved valid in vanadium-catalyzed asymmetric epoxidation of allylic alcohols. The catalyst was then colloidized by delamination in water. The colloidal catalyst was easily separated from the reaction system by simple liquid/liquid separation after catalytic runs and reused without visible loss of catalytic activity and enantioselectivity. But for the heterogeneous catalysts, which were used in solid and separated from the liquid by simple filtration or centrifugation, the recovery and recycle stability need further investigation with respect to multiple non-covalent interactions in their structures. So in this work, the multiple host–guest interactions in the heterogeneous vanadium catalysts using nanosheet-attached α-amino acid anions as chiral ligands have been studied, aiming to explore vigorous and versatile strategies for development of efficient and durable supra-molecular and/or host–guest catalysts.

2. Experimental

2.1. General

All the reagents and chemicals were of analytical purity and used as received from commercial suppliers. The powder X-ray diffraction (XRD) patterns were taken on a Shimadzu XRD-6000 diffractometer with Cu Kα radiation (40 kV and 30 mA) at a scanning rate of 5°/min and step size of 0.02°. The content of Zn, Al, and V was determined on inductively coupled plasma (ICP) atomic emission spectrophotometry (Shimadzu ICPs-7500) by dissolving the samples in dilute HNO_3. The C, H, and N element analysis was performed on an Elementar Co. Vario elemental analyzer. The Fourier transform infrared (FT-IR) spectra were recorded on a Bruker Vector 22 FT-IR spectrometer with a resolution of 4 cm^{-1} using the standard KBr pellet method. The ^{51}V nuclear magnetic resonance (NMR) spectra were obtained with a Bruker AV300 NMR spectrometer at a resonance frequency of 78.90 MHz. The chemical shifts (δ) are referenced to external neat $VOCl_3$. The scanning electron microscope (SEM) and energy dispersive X-ray (EDX) images were taken on a Zeiss Supra 55 scanning electron microscope equipped with an EDX spectroscope. The accelerating voltage applied was 20 kV. The final chemical compositions of the catalysts were determined as $[Zn_{0.60}Al_{0.41}(OH)_2]$(L-glutamate)$_{0.17}(CO_3)_{0.03}\cdot 0.78H_2O$, $[Zn_{0.61}Al_{0.39}(OH)_2]$(L-alanine)$_{0.13}(NO_3)_{0.26}\cdot 0.42H_2O$, and $[Zn_{0.63}Al_{0.37}(OH)_2]$(L-serine)$_{0.13}(NO_3)_{0.24}\cdot 0.24H_2O$ according to the ICP and CHN elemental analysis results.

2.2. Modification of L-glutamate (Glu) with LDH nanosheet

In order to obtain high-quality nanosheets, the Zn/Al—NO_3^-–LDHs was synthesized via ion exchange from Zn/Al—CO_3^{2-}–LDHs instead of direct synthesis. Highly crystallized ZnAl—CO_3^{2-}–LDHs was synthesized through a modified urea hydrolysis method [22]. A mixed solution containing $Zn(NO_3)_2$ (10 mM), $Al(NO_3)_3$ (5 mM), and urea (35 mM) in 320 mL deionized water was agitated at refluxing temperature (100 °C) for 24 h in a three-neck flask. The precipitate white solid was filtered, washed with heated deionized water for six times and anhydrous ethanol two times, and then dried at 50 °C for 12 h. The Zn/Al—NO_3^-–LDHs was prepared by ion-exchange reaction by suspending the Zn/Al—CO_3^{2-}–LDHs crystals (0.4 g) in the solution of HNO_3 (0.062 mol) and $NaNO_3$ (0.62 mol) in decarbonated deionized water (400 mL) and stirred at ambient temperature for 24 h under N_2 atmosphere. The solid was filtered, washed with decarbonated deionized water for six times and anhydrous ethanol two times, and then vacuumed at 40 °C for 12 h. The Zn/Al-Glu-LDHs was prepared through ion-exchange approach using Zn/Al—NO_3^-–LDHs as precursor. First, L-glutamate aqueous solution was adjusted with 1 M aqueous ammonia to pH = 10–10.5 by monitoring with a pH meter and then stirred at ambient temperature for 0.5 h under N_2 atmosphere. Then, Zn/Al—NO_3^-–LDHs was suspended in 15 mL of decarbonated deionized water and mixed with the L-glutamate aqueous solution. The resultant suspension was stirred at ambient temperature for 24 h under N_2 atmosphere and then filtrated. The solid was washed with decarbonated deionized water for six times and anhydrous ethanol two times, and then vacuumed at ambient temperature for 12 h.

2.3. Modification of L-alanine (Ala) and L-serine (Ser) with LDH nanosheet

The Zn/Al-Ala-LDHs and Zn/Al-Ser-LDHs was accomplished through the coprecipitation approach [23] by addition of a mixed solution of 1 M $Zn(NO_3)_2$ and $Al(NO_3)_3$ dropwise to a stirred 50 mM α-amino acid solution (Zn^{2+}/Al^{3+}/α-amino acid molar ratio = 2/1/1). The solution pH was maintained at 9 by dropwise addition of 1 M $NH_3\cdot H_2O$ solution under stirring at 40 °C in N_2 atmosphere for 6 h. The resulting suspension was filtrated, and the solid was washed with decarbonated deionized water for six times and anhydrous alcohol two times and dried in a vacuum oven at room temperature.

2.4. General procedure for the catalytic asymmetric epoxidation of 2-methyl cinnamyl alcohol

Typical experimental procedure for direct asymmetric 2-methyl cinnamyl alcohol catalyzed by heterogeneous vanadium catalyst: 5.0 μL of $VO(OiPr)_3$ (0.02 mmol) and heterogeneous vanadium catalyst (equivalent to 0.02 mmol of α-amino acid) was dispersed in CH_2Cl_2 (1 mL) and $HCONH_2$ (21 mL). After the mixture was stirred for 1 h at 20 °C, 0.6 mL of tert-butyl hydroperoxide (TBHP, 1.59 mmol) in CH_2Cl_2 and 110 μL of 2-methyl cinnamyl alcohol (0.71 mmol) were added. The mixture was stirred at the same temperature for another 24 h. Saturated aqueous Na_2SO_3 was used to quench the reaction, and the mixture was stirred for 1 h at 20 °C and then extracted with ether. The ether phase was dried over Na_2SO_4 and concentrated under reduced pressure.

The conversion of substrate as well as the enantiomer excess (ee) of the epoxidation products transferred onto the epoxy alcohol was evaluated by means of chiral high-performance liquid chromatography (HPLC) analysis on a Varian 210 ProStar fitted with a chiral column (Daciel AD-H) operating under isocratic conditions (0.4 mL/min) using a mobile phase of n-hexane/*i*-propanol (95:5 vol).

3. Results and discussion

3.1. Ligand modification and catalyst reusability

In this work, the nanosheets of LDHs are used to modify chiral α-amino acids, including L-glutamate (Glu), L-alanine (Ala), and L-serine (Ser), by intercalating the α-amino acid anions into the interlayer regions of LDHs. The LDH nanosheet employed here consists of zinc and aluminum hydroxides (Zn/Al-LDHs). The arrangement of interlayer α-amino acid anions has been investigated by XRD patterns. As shown in Fig. 1, a set of 00l diffractions characteristic of hydrotalcite-like structure (Fig. 1, left) are observed for not only nitrate-intercalated Zn/Al-LDHs (Zn/Al – NO_3^--LDHs) as precursor but also all α-amino acid anion intercalated LDHs. The 003 reflection shifts from 10.11° (Fig. 1a) for Zn/Al – NO_3^--LDHs to 7.18° (Fig. 1b) for L-glutamate-intercalated Zn/Al-LDHs (Zn/Al-Glu-LDHs), with the basal spacing increasing from 0.88 to

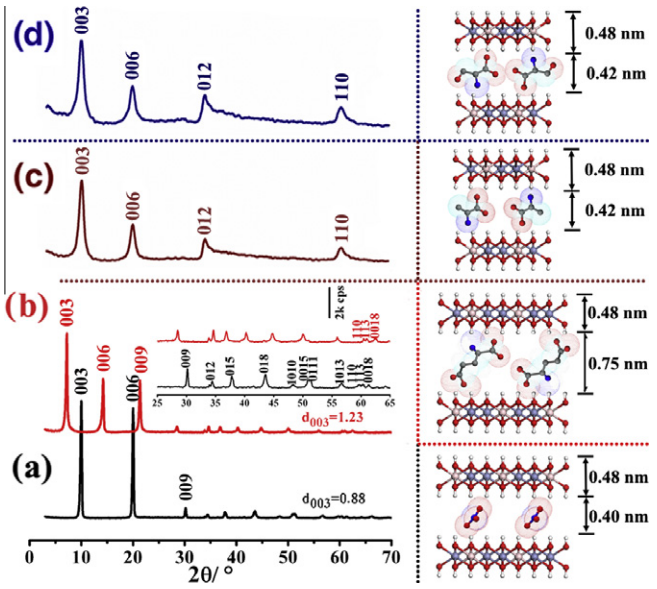

Fig. 1. The XRD patterns (left) and schematic structures (right) of LDHs intercalated with (a) nitrate, (b) L-glutamate, (c) L-alanine, and (d) L-serine anions. Inset: magnification of selected zooms. (Zn Al N C O H).

1.23 nm. The 003 reflection at 9.80° (Fig. 1c and d) for either L-alanine-intercalated Zn/Al-LDHs (Zn/Al-Ala-LDHs) or L-serine-intercalated Zn/Al-LDHs (Zn/Al-Ser-LDHs) gives a basal spacing of 0.90 nm. Subtracting the brucite-like layer thickness (0.48 nm), the interlayer spacing is estimated as 0.75 nm for Zn/Al-Glu-LDHs, 0.42 nm for either Zn/Al-Ala-LDHs or Zn/Al-Ser-LDHs. This refers to a monolayer arrangement of interlayer L-glutamate, L-alanine, and L-serine anions (Fig. 1, right).

The nanosheet-modified α-amino acid anions are then applied as ligands for vanadium centers using $VO(OiPr)_3$ as the precursor of catalytic site. The catalyst recovery and recycling were investigated in vanadium-catalyzed epoxidation of 2-methyl cinnamyl alcohol. In the study, the catalyst was separated by simple filtration and subsequently used without further purification or any treatment. The results are shown in Fig. 2. In either of the ligand-to-V molar ratio of 1/1 (Fig. 2A) or 2/1 (Fig. 2B), the enantioselectivity of major isomer (trans-configured epoxide) has been well preserved in the recycle runs for all the systems using nanosheet-modified L-glutamate, L-alanine and L-serine anion as ligands, and only a slight decreases in the yield were observed in each case. With a ligand-to-V molar ratio of 1 (Fig. 2A), the yield decreased in three catalytic runs from 83 to 80% with nanosheet-modified L-glutamate as ligand (Fig. 2A, a), from 71 to 69% with nanosheet-modified L-alanine as ligand (Fig. 2A, b), and from 81 to 70% with nanosheet-modified L-serine anion as ligand (Fig. 2A, c). With a ligand-to-V molar ratio of 2/1 (Fig. 2B), the yield reduced in the sequence of the heterogeneous vanadium catalysts mentioned above from 18% to 9%, 26% to 23%, and 27% to 22%.

To understand the activity change observed in the recycling runs, the leaching of vanadium and amino acid anions is monitored. With nanosheet-modified L-glutamate, L-alanine and L-serine anion as ligands, 6.6%, 4.2%, and 2.0% of the total vanadium dosage and 25.7%, 0%, and 1.4% of the total α-amino acid anions were leached from the solids in three catalytic runs for the catalyst with a ligand-to-V ratio of 1. The leaching of the vanadium centers into solution and the α-amino acid anions from solids in each catalytic run was also determined and given in Table 1. As shown in Table 1, 2.2%, 1.7%, and 1.4% vanadium centers loss was detected for nanosheet-modified L-glutamate in each catalytic run, 1.1%, 1.7%, and 0.6% loss was detected for nanosheet-modified L-alanine, and 0.3%, 0.8%, and 0.1% loss was detected for nanosheet-modified L-serine. The total vanadium leaching in solution was 5.3%, 3.4%, and 1.2%, respectively, after three catalytic runs. The case was different when it comes to the loss of α-amino acid anions. For nanosheet-modified L-glutamate, 9.6%, 4.1%, and 12.0% loss was observed in each catalytic run. Yet only 1.1% L-serine loss in the first and 0.3% in the second run were detected for nanosheet-modified L-serine, and no L-alanine loss observed in each run for nanosheet-modified L-alanine. Based on the ligand-to-V molar ratio of 1/1, the vanadium leaching with nanosheet-modified L-glutamate as ligand was estimated to all result from the disengagement of α-amino acid anion from LDH nanosheets, and the vanadium leaching with nanosheet-modified L-alanine anion was estimated to all result from the disengagement of vanadium site independently. With nanosheet-modified L-serine anion as ligand, 0.8% vanadium leaching resulted from the disengagement of α-amino acid anion from LDH nanosheets, and 0.4% vanadium was leached independently. As shown in Fig. 3, with nanosheet-modified L-glutamate as ligand, 5.3% vanadium leaching gave rise to a 3% decrease in yield, while with nanosheet-modified L-serine anion as ligand, 1.2% vanadium leaching caused an 11% decrease in yield. The 3.4% vanadium leaching caused a 2% yield reduction with nanosheet-modified L-alanine anion as ligand. It seems that it is the coinstantaneous leaching of vanadium-amino acids species and vanadium center independently that mainly accounts for the yield decrease. For the catalyst with nanosheet-modified L-glutamate as ligand, all the leached vanadium was into the solution together with L-glutamate anions. The vanadium/pristine L-glutamate system was found in our previous work [21] to give excellent yield (99%) in the asymmetric epoxidation of 2-methyl

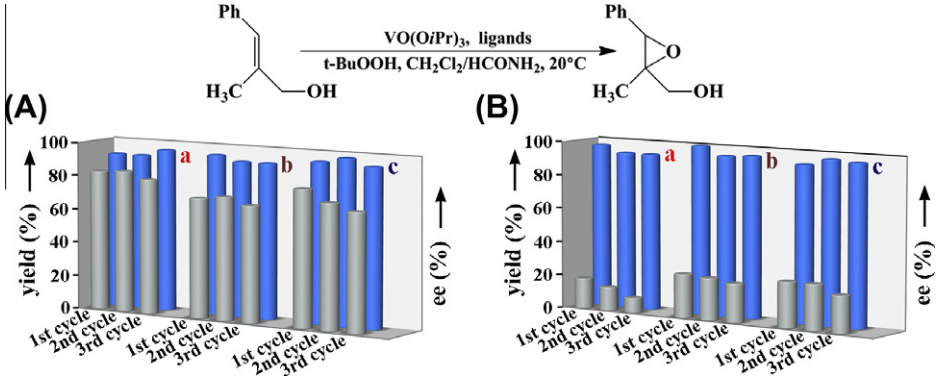

Fig. 2. The yield and ee in the catalytic runs of heterogeneous vanadium catalyst in the epoxidation of 2-methyl cinnamyl alcohol using (a) L-glutamate, (b) L-alanine, and (c) L-serine intercalated Zn/Al-LDHs as chiral ligands with ligand-to-V molar ratio of (A) 1/1 and (B) 2/1 (: yield and : ee_{trans} value).

Table 1
The leaching of vanadium and α-amino acid anions in three catalytic runs.

Ligands		Nanosheet-modified L-glutamate (%)	Nanosheet-modified L-alanine (%)	Nanosheet-modified L-serine (%)
Total vanadium leaching from solids after three catalytic runs		6.6	4.2	2.0
Vanadium leaching in solution in the catalytic runs	1st	2.2	1.1	0.3
	2nd	1.7	1.7	0.8
	3rd	1.4	0.6	0.1
Total vanadium leaching in solution		5.3	3.4	1.2
α-Amino acid anions loss in the catalytic runs	1st	9.6	0	1.1
	2nd	4.1	0	0.3
	3rd	12.0	0	0
Total loss of α-amino acid anions		25.7	0	1.4
Vanadium amount leached with α-amino acid anions		5.3	0	0.8
Vanadium amount leached independently		0	3.4	0.4

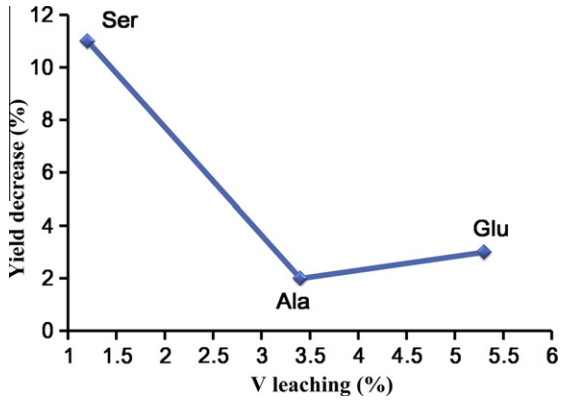

Fig. 3. The relationship between the total V leaching and the yield decrease on the heterogeneous vanadium catalysts using L-glutamate, L-alanine, and L-serine intercalated Zn/Al-LDHs as chiral ligands.

cinnamyl alcohol. That hints, the vanadium centers or L-glutamate anions leached into the solution in V-glutamate species were catalytically active in the epoxidation and could compensate for the activity loss in the recycling experiments in spite of the occurrence of higher L-glutamate leaching. Either the vanadium leaching or the loss of α-amino acid anions is supposed to be associated with the destruction of the interactions between LDH nanosheet and α-amino acid anions and/or the destruction of vanadium–ligand interactions.

3.2. Host–guest interactions between LDH nanosheets and α-amino acid anions

To reveal the reasons for the vanadium leaching and the loss of α-amino acid anions, the nature of the multiple interactions in the vanadium/LDH nanosheet-modified α-amino acid anion systems has been explored by FT-IR spectroscopic characterization and DFT calculations (Fig. 4). In the FT-IR spectrum of Zn/Al-Glu-LDHs, the bands attributed to the asymmetric and symmetric vibrations of carboxylate group in L-glutamate appear at 1593 and 1403 cm^{-1} (Fig. 4A, a), with a $\Delta\upsilon_{COO}$ ($\Delta\upsilon = \upsilon_{as} - \upsilon_{s}$) of 190 cm^{-1}. For Zn/Al-Ala-LDHs, the carboxylate is represented by the absorptions at 1581 and 1354 cm^{-1} (Fig. 4A, b) with a $\Delta\upsilon_{COO}$ of 227 cm^{-1} and at 1583 and 1352 cm^{-1} (Fig. 4A, c) for Zn/Al-Ser-LDHs with a $\Delta\upsilon_{COO}$ of 231 cm^{-1}. Comparing the $\Delta\upsilon_{COO}$ ($\Delta\upsilon_1$) for nanosheet-modified α-amino acid anion with the value of corresponding sodium salt ($\Delta\upsilon_2$) can identify the electrostatic interaction intensity between the brucite-like layer and α-amino acid anions. A larger difference between $\Delta\upsilon_1$ and $\Delta\upsilon_2$ reveals a more diminished symmetry due to a monodentate interaction between carboxylate and brucite-like layer [24,25]. The $\Delta\upsilon_2$ is 156, 213, and 207 cm^{-1} for the sodium salts of L-glutamate, L-alanine, and L-serine [26–28]. Thus, the $\Delta\Delta\upsilon_{COO}(\Delta\upsilon_1 - \Delta\upsilon_2)$ is in the ascending order of 14, 24, and 34 cm^{-1} for nanosheet-modified L-serine, L-alanine, and L-glutamate anions. This indicates that all of the three α-amino acid anions are anchored to LDH layers through monodentate modes and particularly absolute monodentate for L-glutamate. It also means that the electrostatic interaction between L-serine and brucite-like layer is stronger than that between L-alanine and LDH layer, while that between L-glutamate and LDH layer is the weakest. The weakest monodentate electrostatic interactions between LDH layer and intercalated L-glutamate well account for the visible loss (Table 1) of L-glutamate in the catalytic runs. Besides, the H-bonds between the amino acid anions and the LDH layers, a general interaction in hydrotalcite-like structures [29] can be easily formed because of abundant hydroxyl groups on the layer surface. The intense broad absorption band at about 3446 cm^{-1} is due to the H-bond of both the interlayer water molecules and α-amino acid anions with the hydroxyl groups of brucite-like layer. So the molecular modeling combined with DFT calculations has been performed in this work, which is expected to give detailed information on the potential chemical microenvironment between brucite-like layer and α-amino acid anions (Fig. 4B). According to the computational optimization, the lengths of the H-bonds between the two oxygen atoms of carboxylate group in L-glutamate (Fig. 4B, a) and layer hydroxyl are estimated as 0.167 and 0.181 nm. Taking the covalent radius of O^{2-} (0.14 nm) into consideration, the bonding angles between the H-bonds and LDH layers are approximately 57.0° and 50.7°. The intercalated L-alanine shows stronger H-bonding interaction with LDH layers, with bonding lengths of 0.168 and 0.172 nm (Fig. 4B, b) and bonding angles of about 56.4° and 54.5°. The H-bonds between intercalated L-serine and LDH layers are modeled as in the lengths of 0.163 and 0.172 nm, with bonding angles of 59.2° and 54.5° (Fig. 4B, c). It is obvious that stronger electrostatic interactions between brucite-like layer and α-amino acid anions facilitate the formation of stronger H-bonding interactions. The intensities of the H-bonding interactions with brucite-like layers change in a downside trend of L-serine, L-alanine, and L-glutamate.

3.3. Coordination between nanosheet-modified α-amino acid anions and vanadium center

The coordination of nanosheet-modified α-amino acid anions to vanadium center is investigated by the ^{51}V NMR and FT-IR spectroscopy. In the ^{51}V NMR spectra (Fig. 5), the chemical shift in the range of −500 to −600 ppm are assigned [30,31] to the coordination of O and N sites in pristine α-amino acids with vanadium center. The resonance downfield shifts from −553 ppm for the V center coordinated with pristine L-glutamate to −520 ppm for the one coordinated with nanosheet-modified L-glutamate (Fig. 5a) and from −540 to −522 ppm for the vanadium center coordinated with nanosheet-modified L-alanine (Fig. 5b). This results from a greater de-shielding effect on the vanadium center [32] when carboxylic-H was substituted with positively charged LDH layer. But the signal upfield shift from −554 to −588 ppm for the V center coordinated with nanosheet-modified L-serine (Fig. 5c), which means an increasing shielding effect on the vanadium center. The fractional coordination of hydroxyl in L-serine to vanadium center, which is indicated by the shoulder at −523 ppm [33], could be responsible for the increasing shielding effect of nanosheet-modified L-serine.

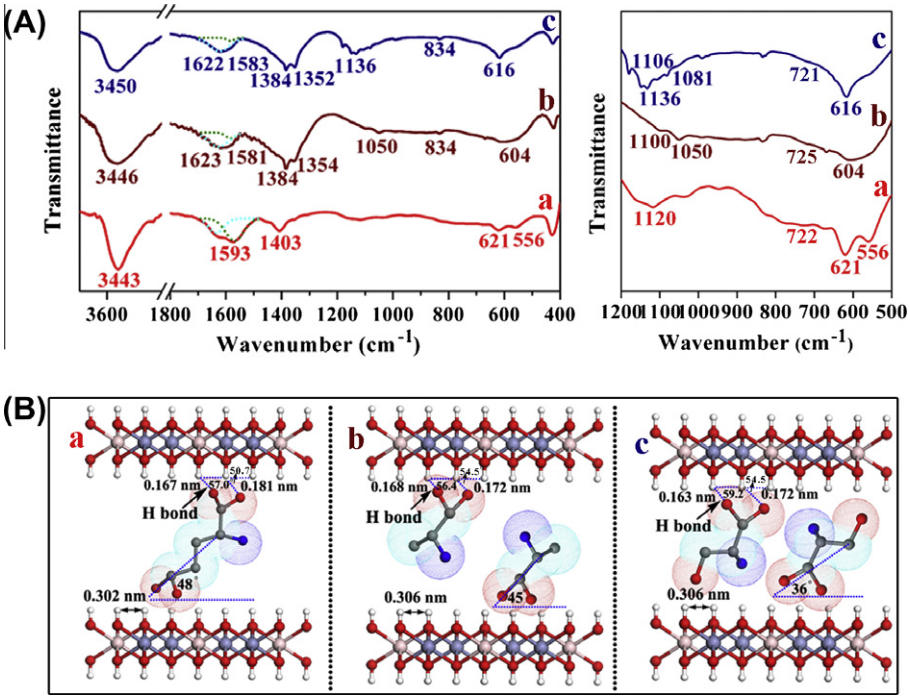

Fig. 4. The FT-IR spectra (A) and calculated H-bonds (B) for (a) Zn/Al-Glu-LDHs, b) Zn/Al-Ala-LDHs, and (c) Zn/Al-Ser-LDHs. The H atoms in α-amino acid anions not involved in the interactions are omitted for clarity. Right part of A: enlarged FT-IR spectra of 1200–500 cm^{-1}. (Zn Al N C O H).

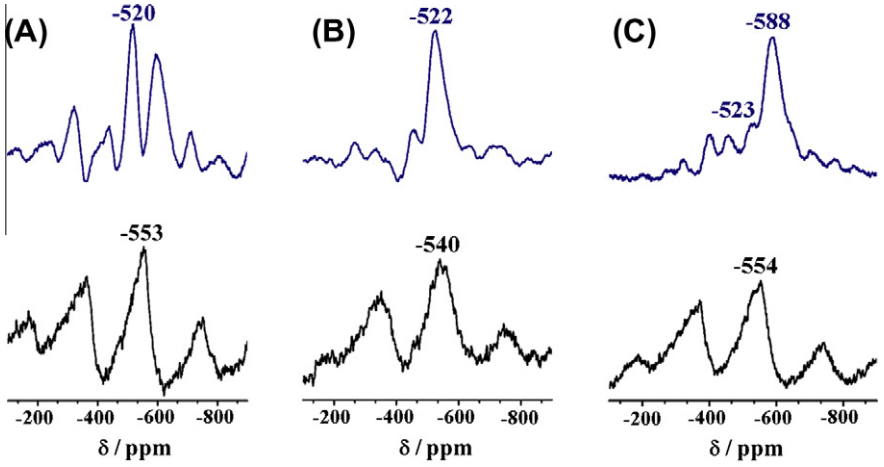

Fig. 5. The ^{51}V NMR spectra for vanadium center from $VO(OiPr)_3$ source, coordinated with intercalated (upper) and pristine (down) (a) L-glutamate, (b) L-alanine, and (c) L-serine.

In the FT-IR spectra (Fig. 6), the absorption bands assigned to V=O stretching vibration and V–N vibration appear at 961 [34] and 567 cm^{-1} for V-Zn/Al-Glu-LDHs (Fig. 6a), at 953 and 556 cm^{-1} for V-Zn/Al-Ala-LDHs (Fig. 6b), and at 959 and 558 cm^{-1} for V-Zn/Al-Ser-LDHs (Fig. 6c), compared with the spectra of right part of Fig. 4A. The band around 556 cm^{-1} can be attributed to the overlapping vibrations of M–O–H bending deformation vibration in LDH nanosheets [35,36] and V–N vibration. But it is not obvious for the nanosheet-modified α-amino acid anion themselves while gets apparently intensive after the coordination of α-amino acid anions to vanadium centers. Meanwhile, the C–N stretching vibration shifts from 1120 to 1070 cm^{-1} ($\Delta\upsilon_{C\text{-}N} = -50$) and N–H out-of-plane vibration [37] from 722 to 749 cm^{-1} for nanosheet-modified L-glutamate, from 1100 to 1059 cm^{-1} ($\Delta\upsilon_{C\text{-}N} = -41$) for V-Zn/Al-Ala-LDHs and from 1108 to 1065 cm^{-1} ($\Delta\upsilon_{C\text{-}N} = -43$) for V-Zn/Al-Ser-LDHs along with the shift of the N–H out-of-plane vibration from 725 and 721 cm^{-1} to 760 and 751 cm^{-1}, further verifying the coordination of the amine-N of nanosheet-modified L-glutamate, L-alanine, and L-serine to vanadium center, which has been observed in the ^{51}V NMR spectrum. But the introduction of $VO(OiPr)_3$ preserved the carboxylate absorptions of nanosheet-modified L-glutamate at 1593 and 1405 cm^{-1} with a $\Delta\upsilon_{COO}$ of 188 cm^{-1}, the carboxylate absorptions of nanosheet-modified L-alanine at 1589 and 1360 cm^{-1} with a $\Delta\upsilon_{COO}$ of 229 cm^{-1}, and the carboxylate absorptions of nanosheet-modified L-serine at 1582 and 1355 cm^{-1} with a $\Delta\upsilon_{COO}$ of 227 cm^{-1}, demonstrating that the coordination with vanadium center has no disruption on the monodentate electrostatic interactions between α-amino acid anions and LDH layers. Obviously, the N atom is the dominating coordination atom

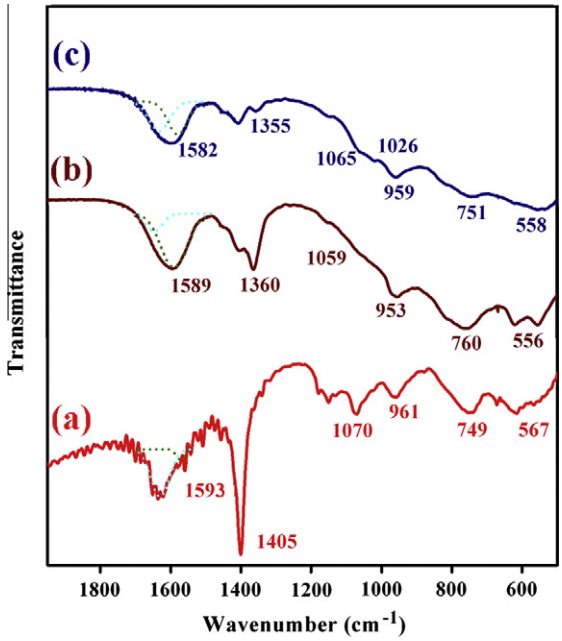

Fig. 6. The FT-IR spectra after the introduction of VO(O*i*Pr)$_3$ as V source to the LDH nanosheet-modified (a) L-glutamate (V-Zn/Al-Glu-LDHs), (b) L-alanine (V-Zn/Al-Ala-LDHs), and (c) L-serine (V-Zn/Al-Ser-LDHs).

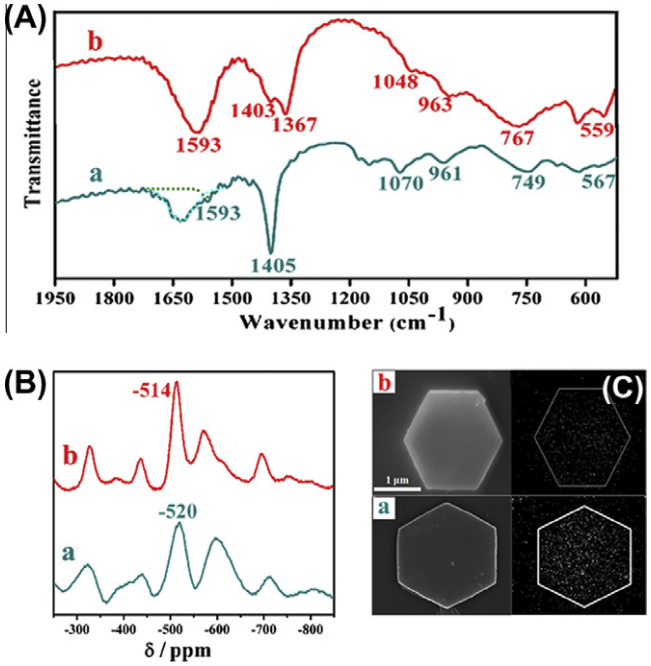

Fig. 8. The FT-IR spectra (A), ^{51}V NMR spectra (B), and SEM (left) and EDX mapping (right) images (C) of (a) fresh and (b) used catalyst with Zn/Al-Glu-LDHs as ligand and VO(O*i*Pr)$_3$ as vanadium source.

because C–N stretching vibrations changed while the asymmetric and symmetric stretching vibrations of carboxylates were scarcely disturbed, which well accords with the bonding distances reported by our group earlier [38]. In light of the difference in the shift of C–N stretching vibrations, the coordination intensity to vanadium center presents an order of L-glutamate > L-serine > L-alanine, which well accounts for the difference in the vanadium amount leached together with α-amino acid anions or independently (Table 1). Stronger coordination with α-amino acid anions caused the vanadium center to be leached independently in less percentage and leached together with α-amino acid anions in more percentage. The higher coordination intensity with L-glutamate provides vanadium center with higher electron density. The higher electron density makes it much easier for the vanadium center to be attacked by the allylic alcohol. This is supposed to contribute to the superior catalytic activity of LDH-modified glutamate system to other amino acid systems (Fig. 2A).

3.4. Relationship between the multiple host–guest interactions and leaching

As shown in Fig. 7, the vanadium amount leached independently due to the destruction of vanadium–ligand interactions decreases gradually with the coordination intensity of vanadium with nanosheet-modified α-amino acid anions (Fig. 7a). But the leaching of α-amino acid anions depends on the dual host–guest interactions. For example, although the electrostatic interaction of brucite-like layer with L-serine is stronger than with L-alanine, the stronger coordination of L-serine to vanadium caused more L-serine to be leached (Fig. 7b).

Taking V-Zn/Al-Glu-LDHs catalyst as an example, the comparison of FT-IR spectra, ^{51}V NMR spectra, and SEM images of the fresh and recovered catalyst convincingly demonstrates that the principal structure remains unaltered after the catalytic runs. Comparing the FT-IR spectrum of the used catalyst in three catalytic runs with that of fresh one (Fig. 8A), it is found that the bands for the asymmetric and symmetric vibrations of carboxylate group in L-glutamate remain at 1593 and 1405 cm^{-1} with a $\Delta\upsilon$ of 188 cm^{-1}, showing no change in monodentate electrostatic interaction between the carboxylate of interlayer L-glutamate and brucite-like layer. The shift of –NH$_2$ out-of-plane vibration from 749 to 767 cm^{-1} and C–N stretching vibration from 1070 to 1048 cm^{-1} indicates a partial leaching of vanadium active center in the catalytic reaction. Meanwhile, the ^{51}V NMR resonance, preserved at nearly the same position (Fig. 8B), indicates the structural

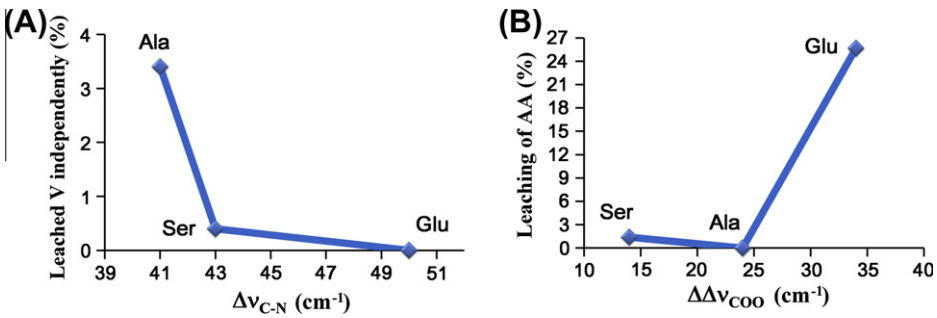

Fig. 7. (a) Leached vanadium independently versus the coordination interaction and (b) leached α-amino acid anions (AA) versus the interactions between LDH nanosheets and α-amino acid anions.

integrity of catalyst after the catalytic runs. Furthermore, the EDX mapping images (Fig. 8C) demonstrate an even distribution of vanadium active center after three catalytic runs.

4. Conclusions

In summary, the investigation on the nature of the multiple interactions in the vanadium/LDH nanosheet-modified α-amino acid anion systems reveals that excellent reusability of heterogeneous supra-molecular catalysts depends on the subtle balance between the multiple non-covalent interactions. The stronger is the coordination with α-amino acid anion, the less is the vanadium center leached independently. But the leaching of α-amino acid anions depends on both of the electrostatic interactions between α-amino acid anions and LDH nanosheets and the coordination interactions between nanosheet-modified α-amino acid anions and vanadium centers. The coordination intensity of nanosheet-modified α-amino acid anions to vanadium center presents an order of L-glutamate > L-serine > L-alanine. All of the vanadium leached together with L-glutamate in nanosheet-modified L-glutamate system while independently in nanosheet-modified L-alanine system. The α-amino acid anions are anchored to LDH layers through monodentate electrostatic interactions in the ascending intensity of L-serine > L-alanine > L-glutamate. The weakest electrostatic interactions lead to the visible loss of L-glutamate in the catalytic runs. The electrostatic interaction of brucite-like layer with L-serine is stronger than with L-alanine, yet the stronger coordination of L-serine to vanadium caused more L-serine to be leached.

Acknowledgments

The authors wish to thank NSFC and 973 Project (2011CBA00504) for financial support. J.H. particularly appreciates the financial aid of China National Funds for Distinguished Young Scientists from the NSFC.

References

[1] Q.-H. Fan, Y.-M. Li, A.S.C. Chan, Chem. Rev. 102 (2002) 3385.
[2] T.J. Dickerson, N.N. Reed, K.D. Janda, Chem. Rev. 102 (2002) 3325.
[3] N.E. Leadbeater, M. Marco, Chem. Rev. 102 (2002) 3217.
[4] J. Dupont, R.F. De Souza, P.A.Z. Suarez, Chem. Rev. 102 (2002) 3667.
[5] C.E. Song, S. Lee, Chem. Rev. 102 (2002) 3495.
[6] D.E. De Vos, M. Dams, B.F. Sels, P.A. Jacobs, Chem. Rev. 102 (2002) 3615.
[7] H.-B. Yu, X.-F. Zheng, Z.-M. Lin, Q.-S. Hu, W.-S. Huang, L.J. Pu, Org. Chem. 64 (1999) 8149.
[8] K.C. Hultzsch, J.A. Jernelius, A.H. Hoveyda, R.R. Schrock, Angew. Chem. Int. Ed. 41 (2002) 589.
[9] H.M. Hultman, M. De Lang, M. Nowotny, I.W.C.E. Arends, U. Hanefeld, R.A. Sheldon, T. Maschmeyer, J. Catal. 217 (2003) 264.
[10] R. Augustine, S. Tanielyan, S. Anderson, H. Yang, Chem. Commun. (1999) 1257.
[11] R. Margalef-Català, C. Claver, P. Salagre, E. Fernández, Tetrahedron-Asymmetry 11 (2000) 1469.
[12] R.M. Gauvin, L. Delevoye, R.A. Hassan, J. Keldenich, A. Mortreux, Inorg. Chem. 46 (2007) 1062.
[13] M.R. Torviso, M.N. Blanco, C.V. Cáceres, J.M. Fraile, J.A. Mayoral, J. Catal. 275 (2010) 70.
[14] S. Abramson, N. Bellocq, M. Laspéras, Top. Catal. 13 (2000) 339.
[15] T. Danelli, R. Annunziata, M. Benaglia, M. Cinquini, F. Cozzi, G. Tocco, Tetrahedron-Asymmetry 14 (2003) 461.
[16] A. Corma, H. Garcia, Adv. Synth. Catal. 348 (2006) 1391.
[17] J.M. Fraile, J.I. García, J.A. Mayoral, Chem. Rev. 109 (2009) 360.
[18] P. McMorn, G.J. Hutchings, Chem. Soc. Rev. 33 (2004) 108.
[19] M. Heitbaum, F. Glorius, I. Escher, Angew. Chem. Int. Ed. 45 (2006) 4732.
[20] J.M. Fraile, J.I. García, J. Massam, J.A. Mayoral, J. Mol. Catal. A 136 (1998) 47.
[21] J.-Z. Wang, L.-W. Zhao, H.-M. Shi, J. He, Angew. Chem. Int. Ed. 50 (2011) 9171.
[22] Z. Liu, R. Ma, M. Osada, N. Iyi, Y. Ebina, K. Takada, T. Sasaki, J. Am. Chem. Soc. 128 (2006) 4872.
[23] S. Aisawa, S. Takahashi, W. Ogasawara, Y. Umetsu, E. Narita, J. Solid State Chem. 162 (2001) 52.
[24] M. Kakihana, T. Nagumo, M. Okamoto, H. Kakihana, J. Phys. Chem. 91 (1987) 6128.
[25] V. Prevot, C. Forano, J.P. Besse, Inorg. Chem. 37 (1998) 4293.
[26] A. Barth, Prog. Biophys. Mol. Biol. 74 (2000) 141.
[27] A.R. Garcia, R.B. De Barros, J.P. Lourenco, L.M. Ilharco, J. Phys. Chem. A 112 (2008) 8280.
[28] T.F. Pauwels, W. Lippens, P.W. Smet, G.G. Herman, A.M. Goeminne, Polyhedron 18 (1999) 1029.
[29] D.G. Evans, R.C.T. Slade, Struct. Bond. 119 (2006) 1.
[30] D. Rehder, C. Weidemann, A. Duch, W. Periebsch, Inorg. Chem. 27 (1988) 584.
[31] V. Vergopoulos, W. Priebsch, M. Fritzsche, D. Rehder, Inorg. Chem. 32 (1993) 1844.
[32] H. Schmidt, I. Andersson, D. Rehder, L. Pettersson, Chem. Eur. J. 7 (2001) 251.
[33] D. Rehder, Inorg. Chem. 27 (1988) 4312.
[34] C. Gabriel, M. Kaliva, J. Venetis, P. Baran, I. Rodriguez-Escudero, G. Voyiatzis, M. Zervou, A. Salifoglou, Inorg. Chem. 48 (2009) 476.
[35] S. Kannan, C.S. Swamy, J. Mater. Sci. 32 (1997) 1623.
[36] Q. Yuan, M. Wei, D.G. Evans, X. Duan, J. Phys. Chem. B 108 (2004) 12381.
[37] P.S. Binil, M.R. Anoop, S.Y. Mary, H.T. Varghese, Y. Panicher, S. Suma, M.R. Sudarsanakumar, Int. J. Ind. Chem. 2 (2011) 1.
[38] L.-W. Zhao, H.-M. Shi, J.-Z. Wang, J. He, Chem. Eur. J. 18 (2012) 9911.